Ultrasound in Med. & Biol., Vol. 25, No. 5, pp. 811–821, 1999

0301-5629/99/$–see front matter

PII S0301-5629(99)00034-4

● *Original Contribution*

ULTRASONIC PROPAGATION IN CANCELLOUS BONE: A NEW STRATIFIED MODEL

ELINOR RUTH HUGHES,* TIMOTHY GRANT LEIGHTON,* GRAHAM WILLIAM PETLEY† and PAUL ROBERT WHITE*

*Institute of Sound and Vibration Research,University of Southampton, Southampton SO17 1BJ UK; and
†Department of Medical Physics and Bioengineering, Southampton University Hospitals NHS Trust, Tremona Road, Southampton SO16 6YD UK

(*Received* 27 *July* 1998; *in final form* 1 *March* 1999)

Abstract—The theoretical modeling of ultrasonic propagation in cancellous bone is pertinent to improving the ultrasonic diagnosis of osteoporosis. First, this paper reviews applications of Biot's theory to this problem. Next, a new approach is presented, based on an idealization of cancellous bone as a periodic array of bone-marrow layers. Schoenberg's theory is applied to this model to predict wave properties. Bovine bone samples were tested *in vitro* using pulses centered at 1 MHz over various angles relative to the orientated cancellous structure. Two longitudinal modes (fast and slow waves) were observed for propagation parallel to the structure, but only one was observed for propagation normal to the structure. Angular-dependence of velocities was examined, and the fast wave was found to be strongly anisotropic. These results gave qualitative agreement with predictions of Schoenberg's theory. Although this new model is a simplification of the cancellous architecture, it has potential for future research. **© 1999 World Federation for Ultrasound in Medicine & Biology.**

Key Words: Ultrasound, Cancellous bone, Osteoporosis, Biot's theory, Schoenberg's theory, Stratified model.

INTRODUCTION AND LITERATURE

Osteoporosis is a skeletal disease characterized by two factors: reduced bone mass and the disruption of the microstructure of bone tissue (Consensus Development Conference 1993). These symptoms increase bone fragility and currently contribute to causing over 60,000 hip fractures in Britain annually. If diagnosed sufficiently early, osteoporosis may be treated effectively to reduce the risk of fracture. The currently preferred diagnostic technique is dual energy x-ray absorptiometry (DXA), which examines bone for one indication of osteoporosis: reduced mass. The second characteristic, the deterioration of the bone microstructure, may potentially be assessed by ultrasonic techniques because this structure is known to affect the transmission of ultrasound (Tavakoli and Evans 1992).

The broadband ultrasonic attenuation (BUA) technique arose following work by Langton et al. (1984). This method measures the frequency-dependent attenuation of ultrasonic pulses, of bandwidth 200–600 kHz, traveling through the os calcis (the heel bone). This skeletal site contains a large amount of cancellous bone; a bony matrix of trabeculae, saturated with marrow. Cancellous bone in the bovine femur is shown in Fig. 1.

Although ultrasound is regarded as a promising tool for bone assessment, being relatively inexpensive, safe and easily utilized, research is still required before it may assist clinical decision-making (National Osteoporosis Society 1996). Systems such as BUA yield a purely empirical measure that has not yet been firmly linked to physical parameters, such as bone strength or porosity. Establishing such relations through a validated predictive model for ultrasonic propagation in cancellous bone would be a significant advance.

This paper reviews one candidate theoretical model, Biot's theory, for application to cancellous bone, and identifies that its isotropic assumption is one of its major weaknesses. A simpler anisotropic layered model of the cancellous architecture is proposed, to which Schoenberg's theory is applied. The predictions

Address correspondence to: Elinor R. Hughes, Fluid Dynamics and Acoustics Group, Institute of Sound and Vibration Research, University of Southampton, Southampton, SO17 1BJ UK. Email: erh@isvr.soton.ac.uk

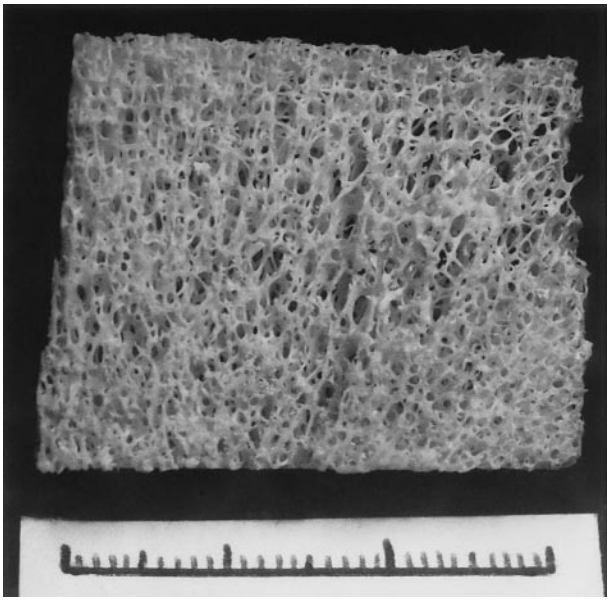

Fig. 1. The porous structure in cancellous bone in the bovine femur. Scale is 3 cm wide, with mm gradings.

of both theories are compared with *in vitro* experiments.

THEORETICAL ASPECTS OF PROPAGATION

The bar equation

A number of theoretical models have been proposed for propagation in cancellous bone. The first assumes that waves travel through cancellous bone with the bar velocity, $V_{bar} = \sqrt{(E/\rho)}$, for Young's modulus, E, and density, ρ, of trabecular material. This equation has been used extensively to predict the elasticity of cortical (compact) bone, useful for quantifying bone strength (Abendschein and Hyatt 1970; Carter and Hayes 1977). It has also been suggested that in a cancellous bone a wave travels along each trabecula with the bar velocity (Rho 1998). However, the authors of the present paper doubt the suitability of the bar equation for ultrasound in cancellous bone. First, it is only valid for macroscopically isotropic media, and cancellous bone is known to be anisotropic. Second, for wavelengths larger than the microstructural dimensions, the bar equation predicts one wave but, for such frequencies in cancellous bone, two waves have clearly been observed (Hosokawa and Otani 1997). Hence, propagation in cancellous bone requires a more detailed explanation than that offered by the bar equation.

Biot's theory

The oversimplified model of the bar equation is contrasted by the complex Biot's theory (Biot 1956a, 1956b), which has been used extensively in geophysical applications. In recent years, Biot's theory has been applied to ultrasound in cancellous bone on a number of occasions (McKelvie and Palmer 1991; Williams 1992; Lauriks et al. 1994; Hosokawa and Otani 1997).

Biot's theory predicts that three waves propagate simultaneously in a fluid-filled porous medium: two compressional waves and one shear wave. The two compressional modes are known as waves of the first and second kind, distinguished by their propagation mechanisms. The wave of the first kind is essentially a bulk wave where fluid and solid are locked together, that usually exhibits negligible dispersion. In wave motion of the second kind, fluid and solid move out-of–phase such that it is usually highly attenuated. The waves of first and second kind are also known as fast and slow waves, respectively. This is because, in practice, the former generally has a greater phase velocity than the latter. However, theoretically, the phase velocity of the wave of the second kind may be greater than that of the first kind under certain conditions (Lawrence and Don 1996). Therefore, the equivalence (first = fast; second = slow) will not be used in this paper until it has been validated.

Acoustic propagation in porous media saturated with fluid (of shear viscosity, η, and density, ρ_f) is divided into low- and high-frequency ranges. These ranges intercept at the critical frequency, ω_{crit}, (Biot 1956a, 1956b), where the viscous skin depth, d_s, is equal to the pore radius, a. In general, for angular frequency, ω, $d_s = \sqrt{(2\eta/\rho_f \omega)}$ is the viscous skin depth. This parameter describes the extent of the viscous shear arising at an interface as fluid flows relative to the solid.

In the low-frequency region of Biot's theory ($\omega < \omega_{\text{crit}}$) (Biot 1956a), a parabolic velocity gradient occurs in the pore fluid because d_s is large compared with the pore size. Viscous coupling locks solid and fluid together, preventing the relative motion associated with slow-wave propagation. Hence, only the fast wave propagates at these frequencies.

In the high-frequency region ($\omega > \omega_{\text{crit}}$) (Biot 1956b), viscous coupling effects decrease as d_s decreases. This yields relative motion between fluid and solid that allows the slow wave to propagate. At these frequencies, viscous coupling effects are dominated by inertial coupling effects that lock fluid and solid together, allowing the fast wave to propagate. Hence, both fast and slow waves propagate in the high-frequency region.

Inertial coupling may be regarded in the following way. When a solid body accelerates in a fluid, it drags an additional mass of surrounding fluid, which may be thought of as a coupled mass. By analogy, during wave motion in a fluid-filled porous solid, an inertial coupling occurs between fluid and solid, represented in Biot's theory by the coefficient, ρ_{12},

$$\rho_{12} = (1 - \alpha)\beta\rho_f, \tag{1}$$

where β is porosity and α is the tortuosity. Equation (1) shows that inertial coupling is related to porosity. It also depends on the geometry of the solid matrix, characterized by the tortuosity, α, although not on the material properties of the solid matrix itself. The tortuosity has been defined for various geometries of porous structure (Berryman 1980) and for dynamics of the fluid (Johnson et al. 1987).

Previous applications of Biot's theory

In the application of Biot's theory to ultrasound in cancellous bone, the interstitial marrow has been assumed to behave as a fluid. This assumption may be made because marrow displays a viscous nature under deformation (Bryant et al. 1989) and has a density similar to that of water.

Rigorous use of Biot's theory requires knowledge of up to 14 parameters. The material parameters required are: fluid and solid densities; bulk moduli of fluid, solid and solid frame; Poisson's ratios of the solid and the frame, and the shear viscosity of the fluid. Structural parameters required are porosity, tortuosity and permeability. The frequency of propagating waves also needs to be known. For cancellous bone, many of these parameters, particularly those of a geometric nature, cannot be easily evaluated *in vitro* or *in vivo*. This represents one of the major difficulties in applying Biot's theory to bone diagnostics.

Using data taken from the literature, the authors calculated that the critical frequency, ω_{crit}, for marrow-saturated cancellous bone was in the region of 1–10 kHz (Hubbuck et al. 1998). This implies that ultrasound (defined as above 20 kHz) will be part of the high-frequency region of Biot's theory, for propagation through this medium. Therefore, two compressional waves should propagate at ultrasonic frequencies in cancellous bone.

Propagation through cancellous bone produces negative dispersion (Nicholson et al. 1996); an observation in quantitative agreement with multiple scattering ideas (Schwartz and Plona 1984). Previous authors generally accepted that the slow wave was highly attenuated, rendering it difficult to observe in practice. Thus, when researchers such as Williams (1992) and Lauriks et al. (1994) reported one compressional wave, it was assumed that this was the fast wave. Although Lakes et al. (1983) reported observing two compressional waves in cortical bone, the lack of the observation of two compressional waves in cancellous bone in earlier research marked a significant omission from evidence supporting the application of Biot's theory. The existence of two compressional waves in this medium was confirmed by Hosokawa and Otani (1997), who were able to obtain agreement between predictions of phase velocity and measurements of both waves.

This paper identifies some important aspects of the above studies. First, although Biot's theory has successfully predicted phase velocity on a number of occasions, there has been a consistent discrepancy between measured and predicted attenuation, possibly owing to a misconception of the meaning of the predicted attenuation. Biot's theory predicts absorption due to viscous losses at internal interfaces only, but experimental measurements record empirical signal loss. Signal loss may include contributions from scattering, absorption of the scattered field, and artefacts of the measurement system, such as diffraction (Xu and Kaufmann 1993) and phase cancellation (Petley et al. 1995). These factors must be known for the comparison between theoretical attenuation and measured signal loss to be meaningful.

The energy of an ultrasonic wave traveling through a porous medium will be partitioned between fast, slow and shear waves. If the attenuation of any wave is to be stated relative to the energy in a single incident pulse, then that partition of energy between shear, fast and slow waves must also be incorporated. If this factor is not taken into account, then simple extrapolations from the degree of attenuation to expected signal amplitude should be critically assessed.

Second, in previous studies, the form of Biot's theory used has assumed that the material is macroscopically isotropic. However, cancellous bone displays anisotropic mechanical and ultrasonic properties (Evans and Tavakoli 1992; Nicholson et al. 1994; Hosokawa and Otani 1998), resulting from a highly oriented trabecular structure in load-bearing bones (Gibson and Ashby 1988). In the following section, an anisotropic model is developed that shows that the observation of compressional modes depends on trabecular orientation. As a codicil, an additional advantage of this model is that it requires specification of fewer bone parameters than Biot's theory.

A STRATIFIED MODEL FOR PROPAGATION IN CANCELLOUS BONE

Models of the trabecular structure

Characterization of the cellular architecture of cancellous bone is necessary to devise suitable mathematical models that may be used to describe its mechanical and ultrasonic properties. Gibson and Ashby (1988) presented idealizations of the trabecular architecture, with mechanical properties originating from an oriented trabecular structure and cellular shapes depending on the loads supported. For equal loads in three axes, equiaxed cells form. For large loading in two directions, cell walls

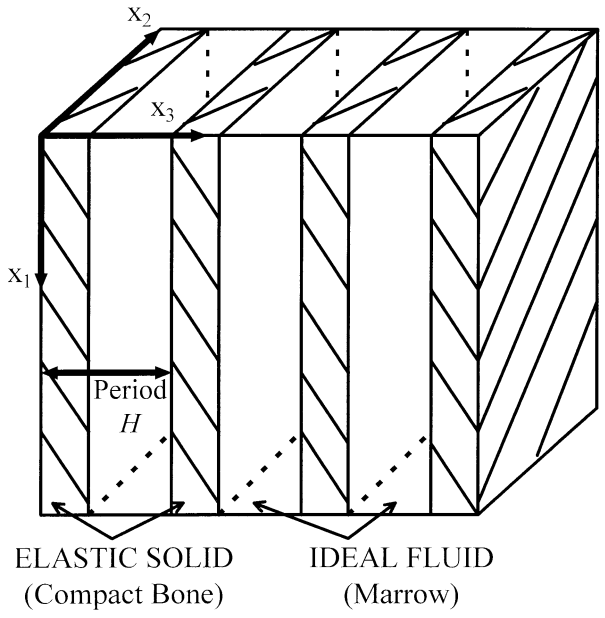

Fig. 2. . An idealization of the architecture of cancellous bone as a series of periodically alternating bone-marrow layers.

align and form a simple layered structure of alternating bone-marrow plates, as in Fig. 2. Although the geometry of this model is highly simplified, it is relatively straightforward to investigate ultrasonic propagation in this system by applying well-established theory of acoustic propagation in strata.

Schoenberg's theory of acoustic propagation in periodic stratified media

Rytov (1956) carried out analysis into wave propagation in periodically layered systems for propagation parallel and perpendicular to stratification. Schoenberg (1984) later presented analysis on propagation in alternating layers in any direction that was verified experimentally by Plona et al. (1987).

In Schoenberg's theory (Schoenberg 1984), the layering is parallel to the x_1 direction, with spatial period H in the x_3 direction (Fig. 2). In one period of a medium with porosity β, the region $0 < x_3 < (1 - \beta)\ H$ is occupied by an elastic solid (that is, it obeys Hooke's Law), with density ρ_s, compressional speed, V_s, and shear speed, V_{sh}. The region $(1 - \beta)\ H < x_3 < H$ contains an ideal fluid, of density, ρ_f, and sound speed V_f. Ideal fluid behavior is a valid assumption for frequencies where the viscous skin depth is much smaller than the fluid layer thickness. In other words, the frequency range covered by Schoenberg's theory corresponds to the high-frequency region of Biot's theory. Furthermore, in practice, to avoid scattering, the wavelength should still be long compared to the period H.

Schoenberg derived the dispersion relation for this medium by relating continuous acoustic field variables in one period to those in the next by propagator matrices. He showed that acoustic wave propagation here could be expressed in terms of a slowness vector, $\mathbf{s} = (s_1, s_2, s_3)$. This vector has magnitude equal to the inverse of phase velocity, with phase angle equivalent to the angle of propagation through the layers relative to stratification. Components of the slowness vector parallel to the layers, s_1, and normal to the layers, s_3, are found from the dispersion relation to be related as

$$\left(\frac{s_3^2}{\langle\rho\rangle}\right) - \left[\frac{\beta(V_f^{-2} - s_1^2}{\rho_f} + \frac{(1-\beta)(V_s^{-2} - s_1^2)}{\rho_s(1 - V_{pl}^2 s_1^2)}\right] = 0, \quad (2)$$

where $\langle\rho\rangle = \beta\rho_f + (1 - \beta).\rho_s$, and V_{pl} is the plate velocity, which can be expressed as

$$V_{pl} = 2(1 - V_{sh}^2/s^2)^{1/2} V_{sh}. \quad (3)$$

Equation (2) can be arranged to give the component normal to the layers, s_3 as a function of those parallel to the layers, s_1. From that relationship, the phase velocity can be found as the inverse of the magnitude of the vector ($|\mathbf{s}| = \sqrt{[s_1^{\ 2} + s_3^{\ 2}]}$) and the propagation angle with respect to the layering ($\theta = \tan^{-1}(s_3/s_1)$).

Schoenberg's theory predicts two compressional waves for all propagation angles, except for that perpendicular to the plates, where there is only one. The two waves are equivalent to the waves of the first and second kind of Biot's theory. Inertial coupling changes with propagation angle relative to the stratification. For propagation parallel to the layers, inertial coupling is zero, and waves may propagate in the fluid and solid independently. Inertial coupling increases with increasing angle, reaching a maximum normal to the layers, where fluid and solid are locked together. This locking impedes the slow wave and only the fast wave propagates.

Fast- and slow-wave velocities were predicted as a function of propagation angle by Biot's theory, eqns (A.1) to (A.8) and values in Table 1, and Schoenberg's theory, eqns (2) and (3) and Table 2. They are plotted in Fig. 3. In this figure, 0° corresponds to the direction perpendicular to the layers and 90° is parallel to the layers. Figure 3 shows that velocities predicted by Biot's theory are constant with angle, unlike those predicted by Schoenberg's theory. From the latter, the fast-wave velocity increases with angle and the slow-wave velocity, being zero at perpendicular incidence, maintains a constant value over a wide angular range. The two theories do, however, give values of velocities parallel to the layers within 10% of each other.

Because many of the parameters for Biot's theory

Table 1. Parameters for Biot's theory.

Parameter	Value
Density of bone, ρ_s	1960 kg/m^3[†]
Density of marrow, P_f	990 kg/m^3[‡]
Young's modulus of bone, E_s	20 GPa*
Bulk modulus of marrow, K_f	2.2 GPa
Shear modulus, N	3.4 GPa[‡]
Poisson's ratio of solid, ν_s	0.32[‡]
Poisson's ratio of frame, ν_b	0.32*
Porosity, β	0.65
Power index, n	1.23*
Viscosity of marrow, η	0.04 Pa.s[§]
Pore radius, a	5×10^{-3} m
Permeability, k_o	5×10^{-9} m^3[‖]
Frequency, f	1 MHz

[†]Lang (1970); [‡]after Duck (1990); *Williams (1992); [§]Bryant et al. (1989); [‖]McKelvie and Palmer (1991).

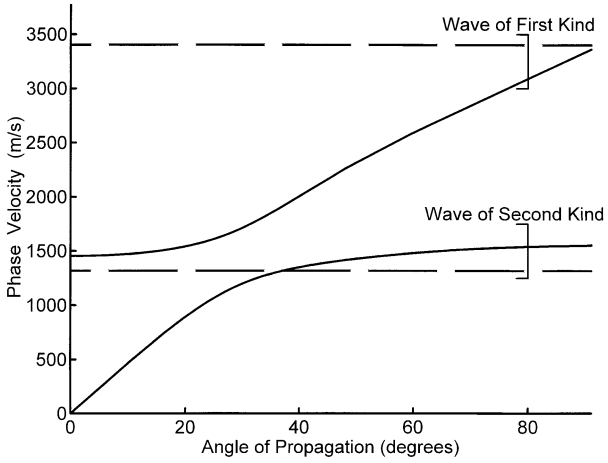

Fig. 3. Predictions of phase velocity against propagation angle for Biot's theory (dashed lines) and Schoenberg's theory (solid lines). 90° corresponds to direction of layers; 0° is perpendicular to layers.

are difficult to evaluate in practice, these predictions will contain errors. Schoenberg's theory requires only six parameters (these being densities, speeds in component media and porosity), which is an advantage for computational issues. In Schoenberg's theory, the fluid is assumed to be inviscid, and so viscous absorption is not predicted. This prevents a direct comparison with absorption predicted by Biot's theory. For this reason, absorption and attenuation are not considered further in this paper. Investigations of fast- and slow-wave phase velocities are presented in the following section.

EXPERIMENTAL SYSTEM AND METHOD

The experiments aimed to observe two compressional waves, to investigate their phase velocities over a range of angles with respect to trabecular orientation, and to compare these results with the predictions of Schoenberg's theory.

Samples of cancellous bone were taken from bovine tibial and femoral epiphyses, known to contain a well-oriented trabecular structure. Specimens of cross-section 30 mm × 30 mm were prepared with the dominant structure extending both parallel and normal to the cross-section, as determined by eye. Sample thickness, measured by micrometer, varied from 0.6 mm to 1.3 mm (± 0.5 mm). The samples were stored in formalin, and the marrow was left intact throughout the experiments.

Two 1-MHz resonance, 2.5-cm diameter transducers were suspended in a water-filled tank, at a separation

Table 2. Parameters for Schoenberg model.

Parameter	Value
Density of bone, ρ_s	1960 kg/m^3[†]
Density of marrow, ρ_f	990 kg/m^3[‡]
Porosity, β	0.65
Solid compressional speed, V_s	3200 m/s*
Fluid compressional speed, V_f	1500 m/s
Shear speed, V_{sh}	1800 m/s[§]

[†]Lang (1970); [‡]Duck (1990); *after Williams (1992); [§]Wu and Cubberley (1997).

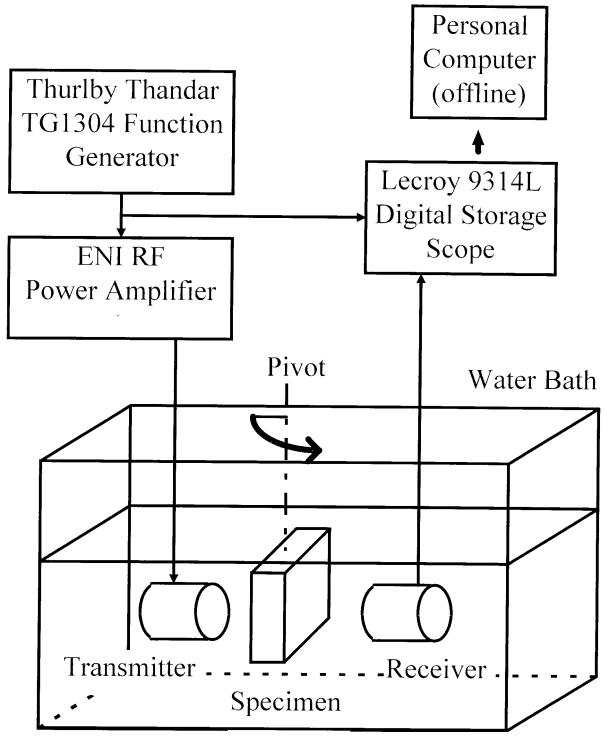

Fig. 4. Schematic diagram of the apparatus used in the experiments.

of 14 cm ± 0.1 cm (Fig. 4). The sample was mounted in an absorbent surround, coaxially aligned between the transducers at a distance of 10 cm ± 0.1 cm from the transmitter. This ensured that it was in the acoustic far field, where plane wave propagation could be assumed over a limited volume. The water temperature was recorded at 20°C ± 0.5°C.

The transmitter was driven by a single sinusoidal pulse of center frequency 1 MHz generated by a signal generator (TG1304, Thurlby Thandar, Ltd., Huntingdon, Cambridgeshire, England), amplified by 50 dB (RF Power Amplifier, ENI, Illinois, USA). Pulses travelled through the water-bone–water path, and were acquired by a digital storage scope (9314L, Lecroy, Chestnut Ridge, N.Y., USA), sampling at 10 MHz over 500 averages. The signal was analyzed off-line on a PC using MATLAB® software.

Data was acquired with the bone specimens in place interrogated initially at normal incidence and, subsequently, with the specimen rotated in the field. Data without the specimen present was recorded as a reference signal.

Calculations

The theories of Biot and Schoenberg predict phase velocity. Therefore, their predictions should be compared with experimentally derived frequency-dependent velocity, and not that derived from pulse transit time. The phase velocity was calculated using a technique developed by Smith (1972) and Plona et. al. (1987) for propagation at any angle of incidence θ_i. This technique uses mode conversion at the fluid-porous solid interface and accounts for refraction through the sample at non-normal angles of incidence. The phase velocity at normal incidence can be expressed as:

$$V_p = V_w/(1 - q), \tag{4}$$

where V_w is the velocity in water and where

$$q = (V_w\phi_b(\omega))/\omega d, \tag{5}$$

where d is the thickness of the target. The term $\phi_b(\omega)$ is the phase difference between pulses with and without the target present. If $F(\omega)$ and $G(\omega)$ are the real and imaginary parts, respectively, of the Fourier transform of signal, the phase may be found as $\phi(\omega) = \tan^{-1}(G(\omega)/F(\omega))$. The phase difference can be expressed in degrees as:

$$\phi_b(f) = (-\phi_w) - (\phi_t) + 360fL_c. \tag{6}$$

In eqn (6), the frequency, f, is in hertz. The phases, in degrees, of pulses received with and without the target present are ϕ_w and ϕ_t, respectively. The term L_c is a time-compensating distance that accounts for the phase of the reference signal in the water displaced by the insertion of the target. For an angle of refraction, θ_r, where:

$$\tan\theta_r = \sin\theta_i(\cos\theta_i - q), \tag{7}$$

the phase velocity can be expressed as:

$$V_p = V_w/(1 + q^2 - 2q\cos\theta_i)^{1/2}. \tag{8}$$

Reproducibility and error

Reproducibility was assessed by testing 6 specimens with trabeculae parallel to the cross-section and 4 with structure perpendicular to this. The procedure was repeated 4 times, with specimens being repositioned each time. Sources of errors in the calculations included the measurement of transducer separation (± 0.5 mm); the width of the sample (± 0.5 mm); the angle of incidence (± 0.5°); and spectral smearing, owing to the truncation in the time domain of the modes being analyzed.

RESULTS

Observation of two compressional waves

Separating propagation modes in the time domain is most easily achieved using pulses, which also allows for temporal windowing for spectral analysis. Figure 5a shows the voltage output trace for a single sinusoidal input pulse, center frequency 1 MHz, traveling between transducers without a specimen present. Figure 5b is the power spectral density of the pulse in Fig. 5a, showing a maximum value around 920 kHz, possibly offset from 1 MHz by nonlinear propagation or dispersion. This spectrum shows the bandwidth of the signal within which it can be assumed that spectral data is reliable and not subject to a poor signal-to–noise ratio.

Figure 6a shows the trace for a 1.2-cm width sample where the trabeculae are parallel to the direction of propagation (referred to here as a parallel sample), interrogated at normal incidence to the surface. Two arrivals can be seen: one of low amplitude around 87 μs, and a prominent arrival around 92 μs (from the time of the trigger). The possibility of these arrivals being reflections from the tank was eliminated because no specular echoes could arrive within the time frame. It was also assumed that no shear wave would be generated at normal incidence, so the arrivals were assumed to be compressional modes travelling through the sample.

To classify the modes in Fig. 6a with respect to waves of Biot and Schoenberg theories, experimental

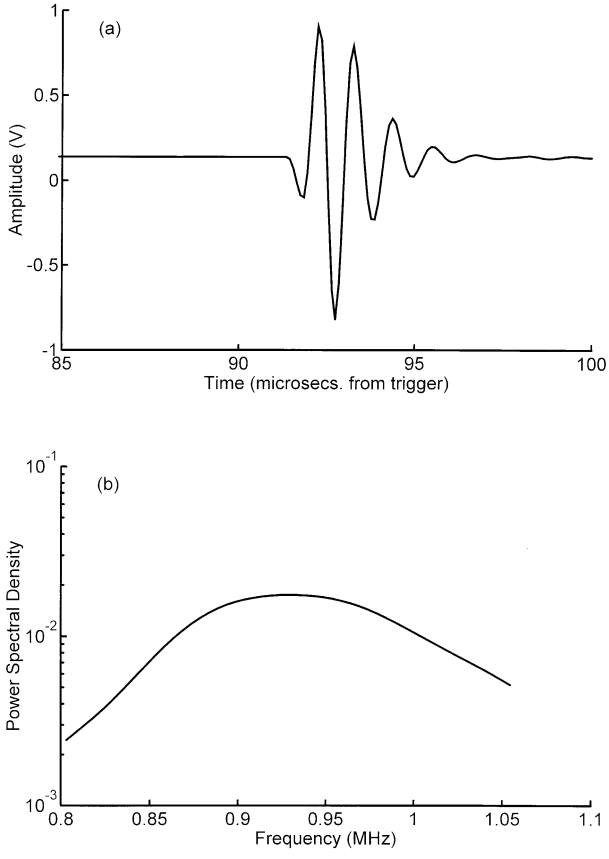

Fig. 5. (a) Time history of 1-MHz center frequency pulse traveling through water bath; (b) its power spectral density.

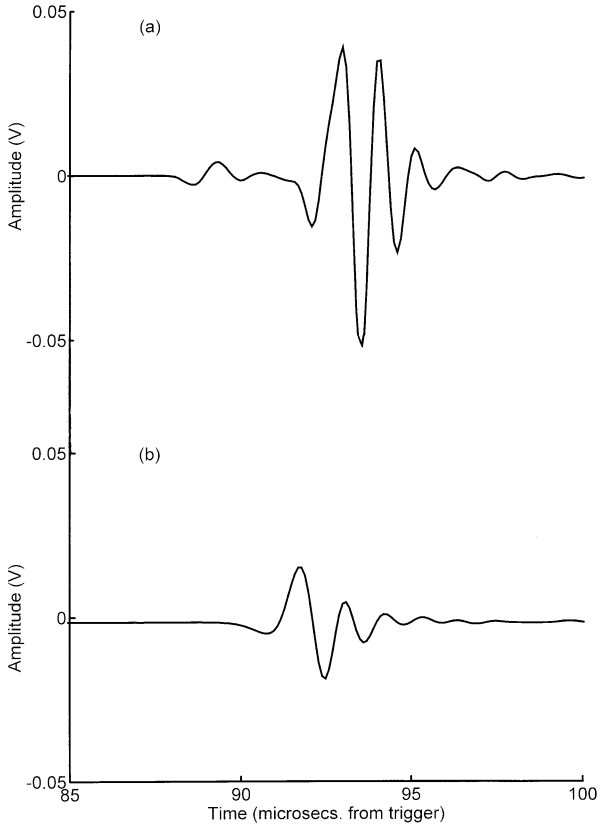

Fig. 6. Time history of 1-MHz pulse traveling through cancellous bone (a) sample of 1.2 cm with structure parallel to propagation direction; and (b) sample of width 1.2 cm with structure normal to propagation direction.

phase velocities were compared with theory (Fig. 7). The phase of each mode was computed using a fast Fourier transform algorithm on a section of the trace. The phase velocity of the pulse in this section was then found using eqns (4) to (6), shown in Fig. 7.

The literature suggests a range of values for bone properties. Using the best-fitting values for bone and marrow within this range (Table 1), the predictions of Biot's theory are shown as solid lines in Fig. 7. It may be argued that it is easy to fit predictions to experimental data, given that Biot's theory has many variables. The authors' unpublished observations suggest that variations in densities and moduli within the literature limits do not appear to significantly alter predicted wave properties. Geometric structural parameters appear to affect wave properties more significantly. Here, porosity is determined by experiment and is, therefore, known. Hence, the fit to experimental data is achieved through changes, within appropriate limits, in those least well-defined parameters, such as permeability and tortuosity.

Figure 7 helps to classify the waves. The arrival at 87 μs gives the upper curve of experimental points that corresponds to the predicted fast wave. The arrival at 92 μs gives the lower curve of experimental points, corresponding to the predicted slow wave. The first arrival will, therefore, be referred to as the fast wave, and the second as the slow wave, for the remainder of this paper. The observation of two compressional modes was repeatable for all parallel samples tested.

Figure 6a shows that the slow-wave amplitude is greater than that of the fast wave in cancellous bone. However, the slow-wave amplitude is generally expected to be less than the fast-wave amplitude, owing to the high attenuation of the former. This discrepancy is likely to be because marrow-filled pores in parallel samples are open to the surrounding reference medium of water. A good acoustic impedance match between water and marrow means motion in the two fluids will couple effectively.

Figure 6b shows the trace emerging for a 1.2-cm wide sample with a trabeculae at right angles to propagation (a perpendicular sample) at normal incidence. (This direction may be thought of as being equivalent to the direction used in current BUA methodology through the calcaneus.) Only one arrival is apparent, which was

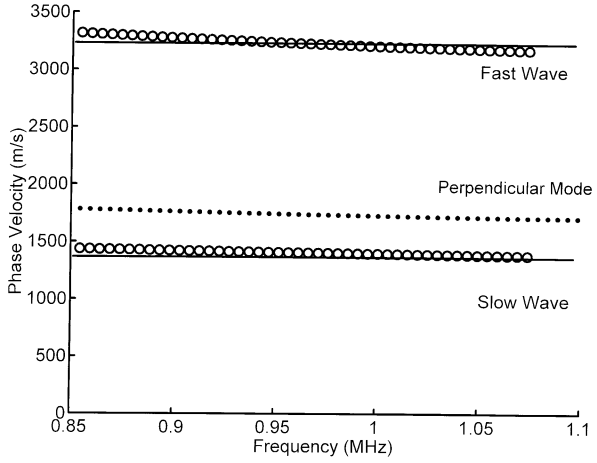

Fig. 7. Phase velocities vs. frequency, showing predictions from Biot's theory (solid lines), observed modes from a parallel sample (○) and mode from perpendicular (•).

found to have propagated through the specimen as a compressional wave. The phase velocity of this mode was evaluated and is plotted in Fig. 7. The experimental points could not be curve-fitted within literature limits to correspond clearly with any predictions from Biot's theory. Therefore, it was not clear whether the mode was a fast or slow wave. This point may be clarified with reference to the stratified model in the following section.

Effect of structural orientation on fast and slow waves

Comparison of Fig. 6a and b clearly shows the influence of trabecular orientation: one mode is observed for the perpendicular sample, compared with two for the parallel sample. To investigate the effect of trabecular orientation further, data were acquired as specimens were pivoted around an axis coaxially aligned with the transducers, which remained fixed. Data were taken for increments in the incidence angle of 5°, over as wide a range as possible before the detection of a signal around the specimen.

Figure 8a and b shows graphs of phase velocity against the angle of refraction, θ_r. Values for θ_r were evaluated at 920 kHz (the frequency of maximum power) using eqns (5) to (8), for each measured angle of incidence, θ_i, sample thickness, d and speed of sound in water, V_w at 20°C. The angle of incidence was evaluated for a particular sample using the convention shown in Fig. 9 and used to plot Fig. 8a and b. This convention defines the angle of incident rays with respect to the trabecular alignment, and not the sample surface.

Phase velocities were predicted for a bone and marrow-layered model using Schoenberg's theory, eqn (2)

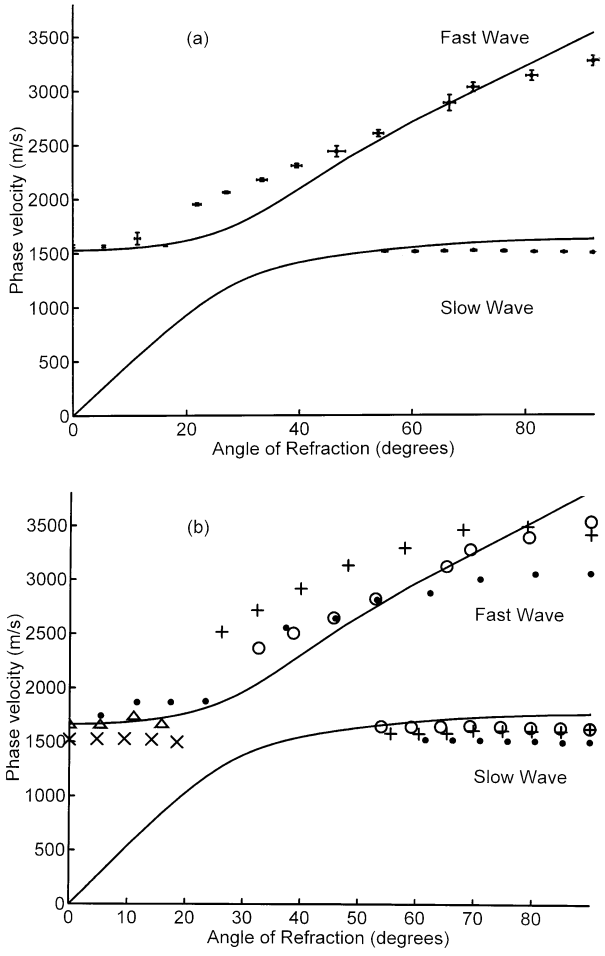

Fig. 8. Phase velocity (at 920 kHz) against angle of refraction with predictions from Schoenberg's theory (solid lines). (a) Accuracy in measurement from one parallel and one perpendicular sample. (b) Reproducibility of measurement in three parallel (symbols +, ○, •) and three perpendicular samples (symbols ×, Δ, •). The trabecular direction is at 90°; 0° is perpendicular to trabeculae.

and Table 2, and are plotted as the solid line in Fig. 8a and b. Where possible, parameter values were the same as for the curve-fitted Biot predictions of Fig. 7.

Figure 8a shows the accuracy in the measurements of physical parameters. Plotted errors include the standard deviation due to spectral smearing (around 5% for fast waves, 2% for slow waves: no larger than the size of the points plotted). The error in the angle of refraction was ± 1°. Having typified the accuracy in this way, these error bars are not shown in Fig. 8b for clarity, which shows errors in terms of reproducibility.

Figure 8a and b, again, shows the anisotropic response of cancellous bone. For refraction angles where the fast wave may be identified (20°–90°), its phase velocity increases with increasing angle. The slow wave

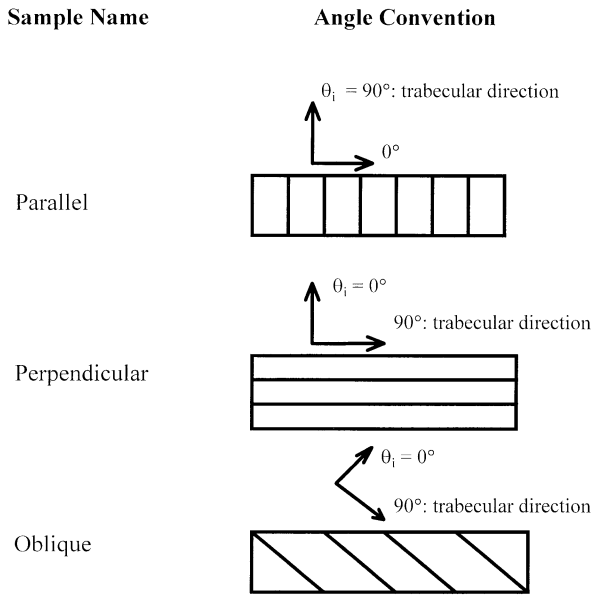

Fig. 9. Angular convention for experimental work and the presentation of results.

is observable over a smaller range (50°–90°) and its phase velocity remains approximately constant for angles where it is observed.

The rate at which the experimentally measured fast-wave velocity changes with angle appears to correspond to that predicted by the Schoenberg model. Similarly, the measured slow-wave velocity, for angles where it was observed, appears to correspond well to the Schoenberg prediction.

Confirmation of compressional wave propagation

Because measurements were taken at non-normal angles of incidence, it was necessary to ensure that shear waves were not being recorded and corrupting the results. To do this, samples with trabecular structure running 45° and 30° to the square cross-section (called oblique samples), were prepared and tested at normal incidence, where it can be assumed shear propagation does not occur.

Phase velocities of waves through the oblique sample gave agreement to within 5% of the data from parallel samples at 45° and 30°. Confidence was, therefore, put in the recording of compressional propagation at non-normal angles.

DISCUSSION

These experiments demonstrate two results. First, the reproducible anisotropic response of fast and slow compressional waves in cancellous bone. Second, evidence that ultrasound in cancellous bone containing a dominant trabecular structure behaves like that in a stratified array of bone-marrow layers. These results are discussed below.

Comparison between Biot's theory and Schoenberg's theory

It is of interest to compare the two theories considered here, and to comment on their respective ability to model propagation in porous bone. The complexity of Biot's theory may mean that it provides a better model conceptually, aside from anisotropic effects, but it is worth considering whether or not it gives significantly better agreement than Schoenberg.

Fluid viscosity is a crucial to Biot's theory because viscous properties define propagation into frequency regions and determine at what frequencies the slow wave may propagate. However, in this version of Schoenberg's theory viscosity is omitted, and the latter theory applies to frequencies where viscous effects can be assumed to be negligible. Results here show that the inclusion of viscosity in Biot's theory gives no significant advantage in agreement with experiment, as when it is omitted by Schoenberg for propagation parallel to the structure.

Replacing interstitial marrow with water in cancellous bone has been known to alter ultrasonic velocity and attenuation *in vitro* (Alves et al. 1996). This may be as a result of marrow having a higher viscosity than water. Furthermore, the viscosity of bovine marrow significantly decreases with an increase in temperature (Bryant et al. 1989) and viscous coupling effects might be expected to decrease *in vivo*. This means that, if viscous coupling is an issue at ultrasonic frequencies, the fast wave may not propagate as effectively at certain propagation angles as it does *in vitro*. Clearly, the effect and role of viscosity in ultrasonic measurements of bone remains uncertain.

Biot's theory, as discussed, assumes that the solid frame is macroscopically isotropic. Anisotropy may be introduced into Biot's theory in two ways: first, in fluid motion within the pores (inertial coupling); and, second, in the bulk modulus of the frame. Under these conditions, Biot's theory may become equivalent to Schoenberg's theory, which further work aims to demonstrate.

Cancellous bone in reality consists of calcified plates that contain perforations and are not impervious, as in the Schoenberg model. Accounting for perforations may improve the accuracy of theoretical predictions, although this may only be further improved after material and structural properties are fully and accurately evaluated.

Implications to in vivo measurement

Diagnostic techniques such as BUA operate in the high-frequency region of Biot's theory where, theoretically, both fast and slow waves propagate. It is, therefore, relevant to discuss the implications of these results *in vivo*.

BUA measurements are taken by transmitting ultrasound through the os calcis (heel) in the mediolateral (widthwise) axis. Trabeculae in the os calcis are aligned in the proximodistal axis (lengthwise), and may be thought to be perpendicular to the direction of propagation in BUA testing. Referring to the Schoenberg model and Fig. 8a and b, this corresponds to propagation perpendicular to layering, where only the fast wave propagates and with a velocity close to 1600 m/s. This may be one reason why there is no evidence of two compressional waves *in vivo*, and why the velocity of observed waves *in vivo* is surprisingly low compared with that for cortical bone (Truscott et al. 1996). The presence of a cortical shell *in vivo* may make the observation of the high amplitude slow waves unlikely, owing to the lack of acoustic coupling between surrounding water and interstitial marrow, as in the *in vitro* case.

The onset of osteoporosis increases the porosity of bone from around 70% to up to 95% (Mellish et al. 1989). Such changes are likely to affect fast and slow wave propagation, owing to a reduction in surface area and, therefore, inertial coupling. However, first order estimates using the Schoenberg model for propagation perpendicular to the trabecular structure (the BUA test configuration) suggest that the velocity may change by less than 5%. Hosokawa and Otani (1998) recently showed that, at high porosity, only one mode in the fluid phase propagates in cancellous bone at ultrasonic frequencies, behavior that, as yet, Biot's theory cannot fully describe.

CONCLUSION

Although the stratified model proposed is clearly a simplification of the cancellous architecture, it may be usefully employed to investigate ultrasonic propagation in cancellous bone. This has given a more in-depth appreciation of the physical and dynamic forces involved in this problem. Uncertainties still exist in the differences between the theories of Biot and Schoenberg; in the role of marrow; and implications to *in vivo* measurement. Nevertheless, this approach has potential for future application in the field of clinical ultrasonic bone assessment.

Acknowledgements—Elinor Hughes (formerly Hubbuck) was financially supported by the Faculty of Engineering and Applied Science at Southampton University. The authors are grateful to Robert Chivers, of the Department of Applied Mathematics and Theoretical Physics, Cambridge University and the Institute of Sound and Vibration Research, Southampton University, for his contribution.

REFERENCES

Abendschein W, Hyatt GW. Ultrasonic and selected physical properties of bone. Clin Orthopaed Related Res 1970;69:294–301.

Alves JM, Ryaby JT, Kaufmann JJ, Magee FP, Siffert RS. Influence of marrow on ultrasonic velocity and attenuation in bovine bone. Calcif Tissue Int 1996;58:362–367.

Berryman JG. Confirmation of Biot's theory. Appl Phys Lett 1980;37: 382–384.

Biot MA. Theory of propagation of elastic waves in a fluid saturated porous solid. I. Low frequency range. J Acoust Soc Am 1956;28: 168–178.

Biot MA. Theory of propagation of elastic waves in a fluid saturated porous solid, II. High frequency range. J Acoust Soc Am 1956;28: 179–191.

Bryant JD, David T, Gaskell PH, King S, Lond G. Rheology of bovine bone marrow. Proc Instn Mech Eng 1989;203:71–75.

Carter DR, Hayes WC. Compressive behaviour of bone as a 2-phase porous structure. J Bone Joint Surg 1977;59:954–962.

Consensus Development Conference. Diagnosis, prophylaxis, and treatment of osteoporosis. Am J Med 1993;94:646–650.

Duck FA. Physical properties of tissue—A comprehensive reference book. Cambridge: Academic Press, 1990.

Evans JA, Tavakoli MB. Temperature and direction dependence of the attenuation and velocity of ultrasound in cancellous and cortical bone. In: Ring, EFJ, ed. Current research in osteo bone mineral measurement. Huddersfield, U.K.:Brit Inst Radiol, 1992.

Gibson LJ. The mechanical behaviour of cancellous bone. J Biomech 1985;18:317–328.

Gibson LJ, Ashby M. Cancellous bone, cellular solids—structure and properties. Oxford: Pergamon Press, 1988;316–331.

Hosokawa A, Otani T. Ultrasonic wave propagation in bovine cancellous bone. J Acoust Soc Am 1997;101:558–562.

Hosokawa A, Otani T. Acoustic anisotropy in bovine cancellous bone. J Acoust Soc Am 1998;103:2718–2722.

Hubbuck ER, Leighton TG, White PR, Petley GW. A theoretical study into factors affecting the Biot slow wave in cancellous bone. ISVR Techn Rep 271, 1998.

Johnson DL, Koplik J, Dashen R. Theory of dynamic permeability and tortuosity in fluid-saturated porous media. J. Fluid Dynamics 1987; 176:379–402.

Lakes RS, Yoon HS, Katz JL. Slow compressional wave propagation in wet human and bovine cortical bone. Science 1983;220:513–515.

Lang S. Ultrasonic method for measuring elastic coefficients of bone and results on fresh and dried bovine bones. IEEE Trans Biomed Eng 1970;17:101–105.

Langton CM, Palmer SB, Porter RW. The measurement of broadband ultrasonic attenuation in cancellous bone. Eng Med 1984;13:89–91.

Lauriks W, Thoen J, Van Asbroek I, Lowet G, Van der perre G. Propagation of ultrasonic pulses through trabecular bone. J Phys 1994;4:1255–1258.

Lawrence DEP, Don CG. Impulse measurements of impedance and propagation constant compared to rigid-frame and dual-wave predictions for foam. J Acoust Soc Am 1996;97:1477–1485.

McKelvie ML, Palmer SB. The interactions of ultrasound with cancellous bone. Phys Med Biol 1991;36:1331–1340.

Mellish RWE, Garrahan NJ, Compston JE. Age-related changes in trabecular width and spacing in human iliac crest biopsies. Bone Min 1989;6:331–338.

National Osteoporosis Society. The use of quantitative ultrasound in the management of osteoporosis. Position Statement of the Scientific Advisory Committee, 16 October 1996.

Nicholson PHF, Haddaway MJ, Davie MWJ. The dependence of ultrasonic properties on orientation in human vertebrae. Phys Med Biol 1994;39:1013–1024.

Nicholson PHF, Lowet G, Langton CM, Dequeker J, Van der Perre G. A comparison of time-domain and frequency-domain approaches to ultrasonic velocity measurement in trabecular bone. Phys Med Biol 1996;41:2421–2435.

Petley GW, Robins PA, Aindow JD. Broadband ultrasonic attenuation—Are current measurement techniques inherently inaccurate? J Radiol 1995;39:1013–1024.

Plona TJ, Winkler KW, Schoenberg M. Acoustic waves in alternating fluid/solid layers. J Acoust Soc Am 1987;81:1227–1234.
Rho JY. Ultrasonic characterisation in determining elastic modulus of trabecular bone material. Med Biol Eng Computing 1998;36:57–59.
Rytov SM. Acoustical properties of a thinly layered medium. Phys Acoust 1956;2:68–80.
Schoenberg M. Wave propagation in alternating solid and fluid layers. Wave Motion 1984;6:303–320.
Schwartz L, Plona TJ. Ultrasonic Propagation in close-packed disordered suspensions. J Appl Phys 1984;55:3971–3977.
Smith RE. Ultrasonic elastic constants of carbon fibres and their composites. J Appl Phys 1972;43:2555–2561.
Tavakoli MB, Evans JA. The effect of bone structure on ultrasonic attenuation and velocity. Phys Med Biol 1992;30:389–395.
Truscott JG, Lightley D, Smith A, Smith MA. Reference ranges for speed of sound and broadband ultrasonic attenuation measured with a Lunar Achilles in 949 Caucasian women. Proceedings of the Bath Conference on Osteoporosis and Bone Mineral Measurement 1996, page 58.
Williams JL. Ultrasonic wave propagation in cancellous and cortical bone: predictions of some experimental results by Biot's theory. J Acoust Soc Am 1992;92:1106–1112.
Wu J, Cubberley F. Measurements of velocity and attenuation of shear waves in bovine compact bone using ultrasonic spectroscopy. Ultrasound Med Biol 1997;23:129–134.
Xu W, Kaufmann JJ. Diffraction correction methods for insertion ultrasound attenuation estimation. IEEE Trans Biomed Eng 1993; 40:563–570.

APPENDIX

Biot's theory predicts two compressional waves (first, second) and one shear wave in a fluid-saturated porous media. The complex velocities of these modes are:

$$V^2_{\text{first, second}} = \frac{\Delta \pm [\Delta^2 - 4(PR - Q^2)(\rho_{11}P_{12} - \rho^2_{12})]^{1/2}}{2(\rho_{11}\rho_{12} - \rho^2_{12})} \tag{A.1}$$

$$V^2_{\text{shear}} = N/[(1 - \beta)\rho_s + (1 - 1/\alpha)\rho_f, \tag{A.2}$$

for $\Delta = P\rho_{22} + R\rho_{11} - 2Q\,\rho_{12}$. The real part of the root gives the phase velocity (m/s), while the attenuation in Np/m, is found from the imaginary part of the wavenumber, which equals $q_{f,\,sl,\,sh} = \omega/\,V_{f,\,sl,\,sh}$. Elastic coefficients, P, Q and R, equal:

$$P = \frac{\beta(K_s/K_f - 1)K_b + \beta^2 K_s + (1 - 2\beta)(K_s - K_b)}{1 - \beta - K_b/K_s + \beta K_s/K_f} + \frac{4N}{3}, \tag{A.3}$$

$$Q = \frac{(1 - \beta - K_b/K_s)\beta K_s}{1 - \beta - K_b/K_s + \beta K_s/K_f}, \tag{A.4}$$

$$R = \frac{K_s\beta^2}{1 - \beta - K_b/K_s + \beta K_s/K_f}, \tag{A.5}$$

where K_f, K_s and K_b are bulk moduli of fluid, solid and skeletal frame, respectively; N is the shear modulus and β is porosity. The Young's moduli of the solid, E_s, and frame, E_b, of cancellous bone may be related by the power law, $E_b = E_s(1 - \beta)^n$, where n depends on the alignment of the structure (Gibson 1985). Bulk moduli of solid and frame may be found as $K_s = E_s/3(1 - 2\nu_s)$ and $K_b = E_b/3(1 - 2\nu_b)$, respectively, for Poisson's ratios of solid and frame, ν_s and ν_b.

The terms ρ_{11} and ρ_{22} are partial densities, defined as $\rho_{11} + \rho_{12} = (1 - \beta)\rho_s$, and $\rho_{12} + \rho_{22} = \beta\rho_f$, for solid and fluid densities ρ_s and ρ_f, respectively. The term ρ_{12} is defined as $\rho_{12} = (1 - \alpha)\beta\rho_f$, where α is the tortuosity. Johnson et al. (1987) gave a frequency-dependent tortuosity, $\alpha(\omega)$, as:

$$\alpha(\omega) = \alpha_\infty + j\eta\beta\left(1 - \frac{4j\alpha^2_\infty k^2_0 \rho_f \omega}{\beta^2\Lambda^2}\right)/\omega\rho_f k_0, \tag{A.6}$$

where α_∞ is a geometric tortuosity, Λ is pore size parameter with permeability, k_o, and viscosity, η.